AUTOMATIC DEPTH ELECTRODE LOCALIZATION IN INTRACRANIAL SPACE

Janis Hofmanis, Valerie Louis-Dorr, Olivier Caspary and Louis Maillard
Research Centre for Automatic Control, Institut National Polytechnique de Lorraine
2, av. de la fort de Haye, Vandoeuvre-les-Nancy, France

Keywords: Electrode localization, SEEG, Coregistration, Matter segmentation, Epilepsy, CT.

Abstract: Localization and precise targeting of depth electrodes in the regions of the human brain is critical for accurate clinical diagnoses and treatment as well as for epileptical source localization and studies of in-vivo electrical propagation. By using magnetic resonance imaging (MRI) combined with computed tomography (CT), the authors present a method based on image processing and object recognition that improves electrode localization in different brain anatomies and matter. This method permits the quantified localization of electrode placements in cortex and white matter, and gives the precise position of each electrode, allowing a more detailed study of intra-cranial electrical stimulation, propagation and properties of conductivity related to the brain. Such methods can be extended to depth-scalp signal analysis using simultaneously registered SEEG and EEG measurements.

1 INTRODUCTION

When investigating the brain processes using stereo electroencephalography (SEEG) (Talairach et al., 1974), the main question is how to relate given measurements with spatio-temporal neural source activity. To do this, it is important to build a model that incorporates all unknown parameters. Using recent studies of simultaneously recorded scalp and intracerebral EEG combining with deep brain stimulation (DBS), it could be possible to relate measurements on scalp and intracerebral activity. However, to build a model, one must know the precise position of the electrodes where DBS is executed. It is also important to understand how the electrical conductivity is affected by white matter, precisely, fibers of axons. To analyse this in detail, we must know which depth electrodes are located in white and which in gray matter. There already exist few studies of depth electrode localization in brain anatomies. Oya (Oya et al., 2009) presented an atlas based on SEEG electrode localization in the amygdala. Ekstrom (Ekstrom et al., 2009) showed how to use MRI, and 2D computational unfolding can localize electrodes in the subregions of the hippocampus and the parahippocampal gyrus. Both these methods concentrate on anatomy structure segmentation and not so much on electrode placements in three dimensional brain space. Miller (Miller et al., 2007) has constructed the Matlab package "Location on Cortex" to help localize subdural electrodes using lateral X-ray images. However, this method enables to apply subdural electrode arrays onto a standardized template brain volume and requires neurologists to pinpoint each electrode position manually. There are also applications like BioImage Suite (Yale University, USA) (Duncan et al., 2004) that allow to edit and place manually multicaptors or grid of electrodes according to their position in CT scan image. This, however, is time-consuming when working with many patients and multicaptors. In this paper, the objective of electrode localization is to develop an automatic routine that finds the origin of each electrode in 3-D CT scan.

1.1 Acquisition Methods

Usually, the collector of electrodes, called multicaptor, consists of 10 or 15 separate electrodes each 2mm wide and 0.8mm in diameter separated by 1.5mm of isolator. For one patient, 10 multicaptors can be implanted, of total from 100 to 150 electrodes. Before surgery of multicaptors, MR imaging (3D SPGR T1 weighted-sequence, TR: 20 ms, TE: 6 ms; matrix 512 X 512, with double injection of gadolinium) is applied

Hofmanis J., Louis-Dor V., Caspary O. and Maillard L..
AUTOMATIC DEPTH ELECTRODE LOCALIZATION IN INTRACRANIAL SPACE.
DOI: 10.5220/0003160204590462
In *Proceedings of the International Conference on Bio-inspired Systems and Signal Processing* (BIOSIGNALS-2011), pages 459-462
ISBN: 978-989-8425-35-5

to obtain the configuration of brain anatomy for particular patients. After implementation, CT with voxel size variating from 0.5 x 0.5 x 0.7 mm to 0.6 x 0.6 x 0.7 mm is done.

2 SEEG ELECTRODE LOCALIZATION IN MATTER

Finding the position of intracranial electrodes and their location with respect to brain matter can be described in three steps: 1. Register the electrodes in CT. 2. Co-register CT and preimplant MRI (find transformation matrix). 3. Do matter segmentation in MRI volume. The final step consists in calculating the electrodes position by use of the transformation matrix. If the boundaries are known, then we can determine each electrode in matter spaces (see Figure 1). The following sections explain these steps in detail.

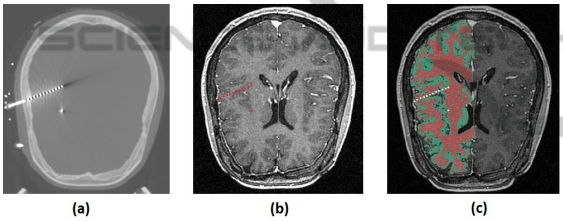

Figure 1: (a) - A slice of a CT image with electrodes, (b) - slice of MRI with approximate position of electrodes (red), (c) - segmented left hemisphere MRI with approximate position of electrodes (white).

2.1 Electrodes Localization in CT Scan

- skull stripping;
- correlation of the pattern;
- identification of the multicaptor;
- optimization of 3D localization.

Each of these steps is explained in detail below.

2.1.1 Skull Stripping

In order to make electrode recognition routines work optimally, extraneous artifacts that do not contain depth electrodes, must be removed from the images. This includes all data outside the skull and intracranial space where multicaptors are located. There are many studies for fast skull stripping in MRI (Dale et al., 1999; Hahn and Peitgen, 2000) and CT scan (Maldjiana et al., 2001; Lee et al., 2008). Suggestions for skull stripping together with implanted depth electrodes was not found. Furthermore, some electrodes can be located in the skull itself, so we need a method for segmenting the area of intracranial space together with the skull. To satisfy these conditions, we developed a procedure based on intensity level thresholding and image morphological processing methods to segment intracranial space. The result of four segmented slices is shown in the Figure 2 below.

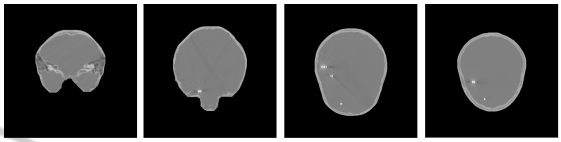

Figure 2: CT image slices after skull stripping.

2.1.2 Correlation of the Pattern

In the next step we apply a 3D correlation to segmented (skull stripped) intracranial volume with a simulated pattern, which is an approximation of one electrode. The retained pattern is a little sphere whose size is determined by the size of the voxel (Figure 3 (b)). We use the spherical object because it has rotation invariant properties and it is more robust in a blurred environment. The correlation of CT scan and pattern gives local maximums (in voxel space), where the pattern matches the electrodes (Figure 3 (c) - red points).

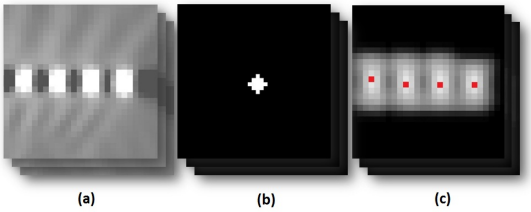

Figure 3: (a) - Blurred electrodes in slice of CT scan, (b) - approximated pattern of electrode, (c) image of correlation result (maximums marked as red points).

Unfortunately, as the mask used for the skull stripping retains some parts of the headholder (which is close to the boundary of the skull), the pattern correlation results in several false maximums that do not correspond to the electrodes, and for some multicaptors, due to angle with CT slice, electrodes were so blurred that correlation produced several maximums for one electrode.

2.1.3 Identification of the Multicaptor

A improved method which correctly interprets the local maximums of the 3D correlation function is proposed for separation and recognition of multicaptors

and recognition of each electrode in these multicaptors. First, this method analyses given local maximum points, detects all sets of points corresponding to the multicaptor and eliminates all other points. This method can be summarized in 7 steps that are repeated until all multicaptors are identified (see chart in Figure 4):

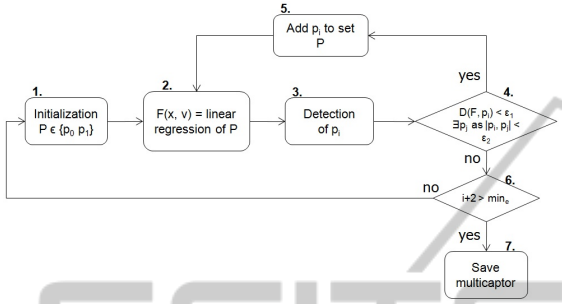

Figure 4: Action diagram of registration of multicaptors.

1. Initialize first points $P = \{p_0, p_1\}$ for multicaptor.
2. Do 3D linear regression as $F(x,\vec{v}) = \underset{x,\vec{v}}{\text{argmin}} \sum_{j=0}^{N-1}[(p_j - F(x,\vec{v}))^2]$, where x and $\vec{v}$ is line's F midpoint and direction vector, respectively, and N is the number of points in set P.
3. Detect $p_i = g_k$, where $g_k = \underset{k}{\text{argmin}}[\mathcal{D}(F, g_k)]$, g is the set of all points and $\mathcal{D}$ is the distance from point g_k to line F.
4. IF $\mathcal{D}(F, p_i) < \varepsilon_1$ AND $\exists p_j \in$P as $\mid p_j - p_i \mid < \varepsilon_2$ DO step 5 ELSE DO step 6. The operator $\mid \cdot \mid$ denotes the vector norm.
5. Add p_i to P and repeat all steps starting form step 2.
6. IF $i+2$ (number of electrodes) $> min_e$ DO step 7 ELSE go to step 1. Here, min_e is minimal electrode amount for one multicaptor (given by neurologists).
7. Save P as multicaptor and remove points of set P from set g.

For the algorithm, we choose value of ε_1 as 5.75mm (this corresponds to one distance and a half between two electrodes alongside) and ε_2 as 2mm (adjusted from a priori knowledge of the mean electrode for 4 patients).

2.1.4 Optimization of 3D Localization

Usually, after the correlation and identification phases, points of multicaptors are not distributed equally on the line and have some shifts along different directions. Therefore, the electrodes of one multicaptor need to be corrected according to the real electrode position with a priori knowledge of the space between electrodes. This is carried out by minimizing the error function for each multicaptor set P found in the previous subsection:

$$F_{error}(\delta) = \sum_{j=1}^{N} \underset{i}{\text{argmin}} \mid p_i - s_j - \delta \mid, \qquad (1)$$

where $S = \{s_0, s_1, \ldots, s_M\}$ is the simulated real multicaptor with M referring to the number of the equally spaced electrodes in the same direction as the multicaptor $P = \{p_0, p_1, \ldots, p_N\}$. The δ is the shifting variable in direction of the multicaptor and $\mid \cdot \mid$ is the vector norm. Thus we calculate the sum of errors (distance between real and simulated points of electrodes) for which we find the global minimum that corresponds best to the real multicaptor.

2.2 CT and MRI Co-registration

Considering that electrodes are localized correctly in post-surgery CT scan, to know their location according to matter, two images, CT and MRI, co-registration must be taken. We resort to Statistical Parametric Mapping 8 toolbox for Matlab (Trust Centre for Neuroimaging, UK) in order to register post-implanted CT with pre-implanted MRI. Registration is achieved by adjusting the relative position and orientation until the mutual information between the images is maximized (Wells et al., 1996; Collignon et al., 1995):

$$\hat{T} = \arg\max_{T} I(u(x), v(T(x))), \qquad (2)$$

where, u is the reference (template) and v is the test volume (image), x - the random variable of coordinates for the voxel, T is a transformation of the coordinate frame of the reference volume into the test volume and I is mutual information between two volumes.

2.3 Matter Segmentation in MRI

The final step is labeling the electrode position with respect to brain matter (white or gray). In the studies of matter segmentation, several recent methods have been presented. Hidden Markov Chain models (Bricq et al., 2008) or Expectation Maximization algorithm (Dugas-Phocion et al., 2004) can be used to segment 3D data. But in the context of this paper we do not search for the best performance segmentation but for the most efficient implementation. So, surface-based

pipeline method (Dale et al., 1999; Hahn and Peitgen, 2000) introduced in FreeSurfer (Martinos Center for Biomedical Imaging, USA) is applied.

The segmentation stage allows to extract the topology of gray/white matter with respect to the position of each electrode.

3 RESULTS

Four patients underwent MR imaging studies prior to depth electrode placement (the number of multicaptors for the first patient was 10, for the second - 11, the third - 9, and the fourth - 8), altogether 456 electrodes. In those 4 cases CT scan was made to track the electrode positions. In all CT scans, electrodes were noticeably blurred and artifacts of wires, holding frames, were visible. Successful skull stripping was carried out. After applying correlation with pattern to CT, not only true but also many false electrode points were calculated. Mainly the false maximum were located in the area of end of the multicaptors and in the headholders. Nevertheless, all multicaptors were found and center of electrodes were located. Due to the end of the multicaptor artifact, the algorithm provides 14 false electrodes additionally. However, for each multicaptor, the number of electrodes is known, and false electrodes can be eliminated automatically. Once the electrodes had been identified, each patient's MRI and CT co-registration were computed, and then, transformations of the electrode positions were calculated. Finally, matter segmentation was applied respectfully of the gray/white matter.

4 CONCLUSIONS

The electrode localization in the matter can be applied automatically (except in few minor cases at segmentation stage). A electrode recognition in CT scan image, and a register of MRI together with CT was done. Lastly we segment the matter and calculate the electrode's position in the brain matter. We put forward a new approach for automatic electrode localization in CT and used some already developed techniques which presented the full circle of automatic depth electrode localization in the brain matter. This proposed method is preprocessing stage of forward modeling within the framework of electrophysiological propagation in cerebral structures.

REFERENCES

Bricq, S., Collet, C., and Armspach, J. (2008). Unifying framework for multimodal brain MRI segmentation based on Hidden Markov Chains. *Medical Image Analysis*, 12(6):639–652.

Collignon, A., Maes, F., Delaere, D., Vandermeulen, D., Suetens, P., and Marchal, G. (1995). Automated multi-modality image registration based on information theory. *Information Processing in Medical Imaging*, 1(1):263–274.

Dale, A., Fischl, B., and Sereno, M. (1999). Cortical surface-based analysis. i. segmentation and surface reconstruction. *Neuroimage*, 9:179–194.

Dugas-Phocion, G., Ballester, M., Malandain, G., Lebrun, C., and Ayache, N. (2004). Improved EM-based tissue segmentation and partial volume effect quantification in multi-sequence brain MRI. *Medical Image Computing and Computer-Assisted Intervention*, pages 26–33.

Duncan, J., Papademetris, X., Yang, J., Jackowski, M., Zeng, X., and Staib, L. (2004). Geometric strategies for neuroanatomic analysis from mri. *Neuroimage*, 23:34–45.

Ekstrom, A., Suthana, N., Behnke, E., Salamon, N., Bookheimer, S., and Fried, I. (2009). High-resolution depth electrode localization and imaging in patients with pharmacologically intractable epilepsy. *Stereotactic and Functional Neurosurgery*, 4(108):812–815.

Hahn, H. and Peitgen, H. (2000). The skull stripping problem in mri solved by a single 3d watershed transform. *Medical image computing and computer-assisted intervention*, 1935:134–143.

Lee, T., Fauzi, M., and Komiya, R. (2008). Segmentation of ct head images. *BioMedical Engineering and Informatics*, 2:233–237.

Maldjiana, J., Chalelaa, J., Kasnera, S., Liebeskinda, D., and Detrea, J. (2001). Automated ct segmentation and analysis for acute middle cerebral artery stroke. *American Journal of Neuroradiology*, 22:1050–1055.

Miller, K., Makeig, S., Hebbb, A., Raoc, R., Dennijs, M., and Ojemannb, J. (2007). Cortical electrode localization from x-rays and simple mapping for electrocorticographic research: The location on cortex (loc) package for matlab. *Journal of Neuroscience Methods*, 162:303–308.

Oya, H., Kawasaki, H., Dahdaleh, N., Wemmie, J., and Howard, M. (2009). Stereotactic atlas-based depth electrode localization in the human amygdala. *Stereotactic and Functional Neurosurgery*, 4(87):219–228.

Talairach, J., Bancoud, J., Szikla, G., Bonis, A., Geier, S., and Vedrenne, C. (1974). New approach to the neurosurgery of epilepsy. stereotaxic methodology and therapeutic results. 1. introduction and history. *Neurochirurgie*, 20:1–240.

Wells, W., Viola, P., Atsumi, H., Nakajima, S., and Kikinis, R. (1996). Multi-modal volume registration by maximisation of mutual information. *Medical Image Analysis*, 1(1):35–51.